Computer-Aided Volumetry of Pulmonary Nodules Exhibiting Ground-Glass Opacity at MDCT

Seitaro Oda[1]
Kazuo Awai[1]
Kohei Murao[2]
Akio Ozawa[2]
Yumi Yanaga[1]
Koichi Kawanaka[1]
Yasuyuki Yamashita[1]

OBJECTIVE. The purpose of this study was to investigate the accuracy and reproducibility of results acquired with computer-aided volumetry software during MDCT of pulmonary nodules exhibiting ground-glass opacity.

MATERIALS AND METHODS. To evaluate the accuracy of computer-aided volumetry software, we performed thin-section helical CT of a chest phantom that included simulated 3-, 5-, 8-, 10-, and 12-mm-diameter ground-glass opacity nodules with attenuation of –800, –630, and –450 HU. Three radiologists measured the volume of the nodules and calculated the relative volume measurement error, which was defined as follows: (measured nodule volume minus assumed nodule volume ÷ assumed nodule volume) × 100. Two radiologists performed two independent measurements of 59 nodules in humans. Intraobserver and interobserver agreement was evaluated with Bland-Altman methods.

RESULTS. The relative volume measurement error for simulated ground-glass opacity nodules measuring 3 mm ranged from 51.1% to 85.2% and for nodules measuring 5 mm or more in diameter ranged from –4.1% to 7.1%. In the clinical study, for intraobserver agreement, the 95% limits of agreement were –14.9% and –13.7% and –16.6% to 15.7% for observers A and B. For interobserver agreement, these values were –16.3% to 23.7% for nodules 8 mm in diameter or larger.

CONCLUSION. With computer-aided volumetry of ground-glass opacity nodules, the relative volume measurement error was small for nodules 5 mm in diameter or larger. Intraobserver and interobserver agreement was relatively high for nodules 8 mm in diameter or larger.

Keywords: computer-aided diagnosis, ground-glass opacity, high-resolution CT, pulmonary nodules, volumetry

DOI:10.2214/AJR.09.2583

Received February 14, 2009; accepted after revision July 19, 2009.

The employment status of K. Murao and A. Ozawa at Fujitsu did not influence the data in this study.

[1]Department of Diagnostic Radiology, Graduate School of Medical Sciences, Kumamoto University, 1-1-1 Honjyo, Kumamoto 860-8556, Japan. Address correspondence to S. Oda.

[2]Bio-IT Business Development Group, Fujitsu, Tokyo, Japan.

AJR 2010; 194:398–406

0361–803X/10/1942–398

Among pulmonary nodules detected at lung cancer screening with low radiation dose helical CT (low-dose CT), 19–38% exhibit focal ground-glass opacity (GGO) [1, 2]. Nodules exhibiting GGO (GGO nodules) may be attributable to focal inflammation, focal interstitial fibrosis [3], atypical adenomatous hyperplasia [4, 5], bronchioloalveolar carcinoma (BAC) [4–6], or adenocarcinoma [4–6]. Although important, differentiation of BAC and adenocarcinoma, which are malignant, from other diseases can be difficult on a single CT scan [7]. Although many inflammatory lesions resolve spontaneously or with antibiotic treatment [5], the size of GGO nodules attributable to BAC or adenocarcinoma gradually increases [8–10]. Focal interstitial fibrosis and atypical adenomatous hyperplasia with pure GGO remain stable in size for months or years [3]. Therefore, monitoring nodule size for several months with high-resolution CT may help in differential diagnosis. Because the doubling time of BAC is long (average, 457–813 days) [8, 11], subjective evaluation of the growth rate by radiologists is unreliable.

With MDCT it is possible to scan a wide range, including areas containing pulmonary nodules, at a detector collimation of 0.500–0.625 mm in one breath-hold. This capability facilitates 3D evaluation of pulmonary nodules. In previous studies [12–16], investigators assessed computer-aided volumetry of pulmonary nodules using volumetric data obtained at MDCT, and the technique reportedly had sufficiently high accuracy and reproducibility [12]. In those studies, however, only solid pulmonary nodules were evaluated with the software used, and computer-aided volumetry of GGO nodules reportedly was difficult [15]. We developed computer-aided volumetry software that can be used to measure the volume not only of solid but also of

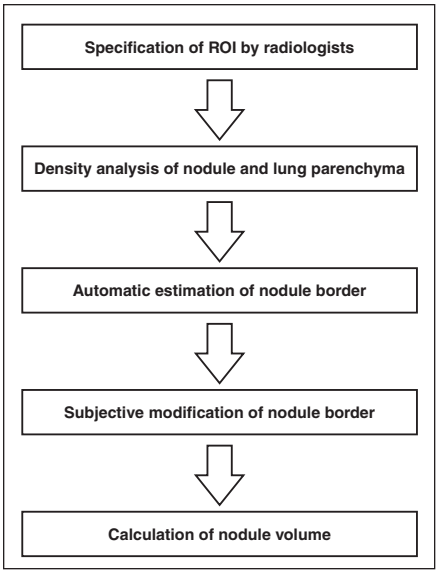

Fig. 1—Diagram of computerized scheme for volumetry of nodules on thin-section helical CT images. ROI = region of interest.

GGO nodules. The purpose of this study was to investigate the accuracy and reproducibility of results obtained on GGO nodules with our computer-aided volumetry software.

Materials and Methods

Computerized Volumetry of Pulmonary Nodules

For volumetry of GGO nodules (Figs. 1 and 2), we used prototype software developed for a PACS (3D analysis software for HOPE/DrABLE-EX, Fujitsu). First, with a single click-and-drag maneuver, the radiologists roughly specified the region of interest to include the target nodule on axial, sagittal, and coronal images. In an improvement of our previously reported method [17], the nodule was automatically segmented with the computer-aided volumetry software. For robust extraction of nodules from the lung parenchyma, we adopted an adaptive threshold attenuation value based on the attenuation value of the target nodule and the lung parenchymal background. When the difference between the attenuation value of the target nodule and that of the lung parenchyma was relatively large, the computer-aided volumetry software chose the threshold attenuation value that approximated the mean value of the nodule and lung parenchyma. When the difference in the attenuation value of the nodule and lung parenchyma was relatively small, the threshold attenuation value nonlinearly approached the average attenuation value of the lung parenchyma.

In the pulmonary nodule extraction process, structures connected to the nodule, such as vessels and bronchi, were roughly eliminated by the computer-aided volumetry software. Occasionally, some structures remained around the nodules (Fig. 2C), or part of the nodule was not included in the extracted area. In such cases, the radiologists who performed volumetry used the mathematic morphology erosion–dilation technique to edit the segmented area to include the nodule by changing the threshold level that separated the density of the nodule from the base density of the lung [18] (Fig. 2D). Erosion–dilation is a useful digital image-processing technique for eliminating structures tangent with the nodule, such as vessels and thoracic wall. Because it was based on the subjective judgment of each radiologist, this modification resulted in volumetric intraobserver and interobserver discrepancies.

Although the prototype software allows freehand shape editing, the radiologists were not allowed to use this technique. Rather, they could use only the aforedescribed image-processing technique to assure the reproducibility of segmentation. The judgment of successful segmentation was based on the observers' visual assessment on axial CT images and on sagittal and coronal multiplanar reconstructed images. Finally, the volume of the segmented area was automatically measured with the software. The average calculation time required by the computer-aided volumetry system to analyze each nodule was less than 1.0 seconds. A computer workstation (FMV-H8230, Fujitsu) with dual 2.16-GHz processors (Core Duo, Intel) was used in this study.

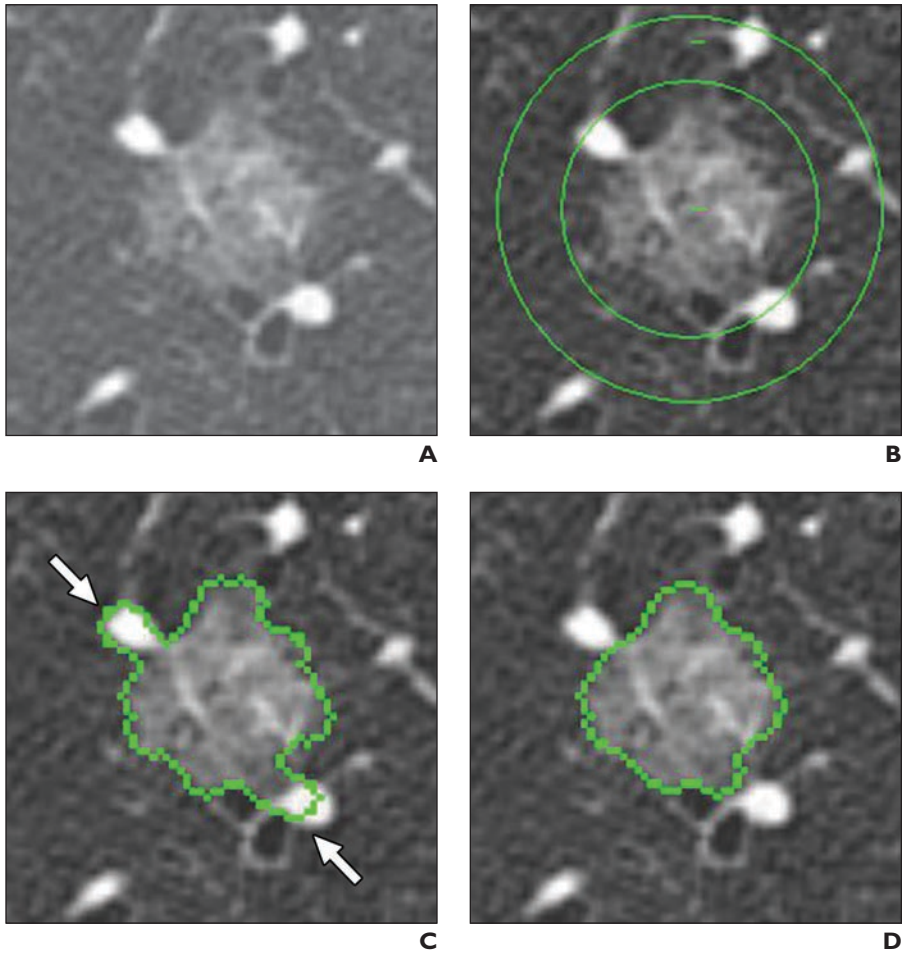

Fig. 2—62-year-old woman with bronchioalveolar carcinoma. Computerized scheme for volumetry of nodules on thin-section helical CT images.
A, High-resolution CT scan shows target ground-glass opacity nodule.
B, High-resolution CT scan shows target ground-glass opacity nodule specified by and place region of interest manually placed by radiologists.
C, High-resolution CT scan shows density of nodule and surrounding lung parenchyma automatically analyzed with software and nodule border estimated. Structures such as vessels occasionally remained around nodules (*arrows*).
D, High-resolution CT scan shows nodule border subjectively modified by radiologists using semiautomatic edit tool and concept of mathematic morphology. Nodule volume is automatically calculated with software.

Phantom Study

Chest phantom—To evaluate the accuracy of our computer-aided volumetry software, we conducted a phantom study with simulated GGO nodules. Ours was a commercially available chest CT phantom with simulated GGO nodules (multipurpose chest phantom N1, Kyoto Kagaku). In this phantom, simulated soft tissues, such as pulmonary vessels, the chest wall, heart, diaphragm, and liver, consist of polyurethane resin composites, and simulated bone consists of an epoxide resin. The space between the pulmonary vessels, heart, and chest wall was filled with air. The chest wall can be removed from the other structures, such as the simulated heart, pulmonary vessels, diaphragm, and liver. Simulated nodules were spheres made of urethane foam resin. The diameters of the simulated nodules were 3 mm (estimated error, 20%), 5 mm (estimated error, 6%), 8 mm (estimated error, 4%), 10 mm (estimated error, 3%), and 12 mm (estimated error, 2.5%), and the attenuation values of the simulated nodules were –800, –630, and –450 HU. On CT scans of the chest phantom harboring simulated nodules, we placed a nodule on bifurcations of the pulmonary vessels in the right lung at the level of the carina.

CT of phantom—CT was performed with a 64-MDCT scanner (Brilliance 64, Philips Healthcare). The scanning parameters were detector row width, 0.625 mm; helical pitch, 0.673; section thickness and section interval, 1 mm; rotation time, 0.5 second; tube voltage, 120 kVp; tube current, 250 mAs.

Volumetry of simulated GGO nodules—Figure 3 shows the screen display of the computer-aided volumetry software in the phantom study. Three radiologists with 4-, 10-, and 15 years of experience in chest CT subjected each simulated nodule to three volumetric measurements, and the resultant values were averaged for each nodule. Each radiologist performed three volumetry sessions at 1-week or longer intervals. We calculated the relative volume measurement error for each nodule to evaluate the accuracy of our volumetry software. The error was defined as follows: [(measured nodule volume – assumed nodule volume) ÷ assumed nodule volume] × 100. The assumed nodule volume was the calculated volume based on the diameter of a simulated spherical nodule. We calculated the mean relative volume measurement error for each nodule by averaging the values reported by the three radiologists.

Clinical Study

To evaluate the reproducibility of our computer-aided volumetry software, represented by intraobserver and interobserver agreement, we conducted a study using data derived from patients. We also investigated whether the need for editing the segment area or the edit time depends on the morphologic features of the GGO nodule. All patients who underwent CT examinations at our institution had given prior informed consent for the use of their CT images in future retrospective studies. Our institutional review board approved the use of the CT database. The requirement for informed specific study-related consent was waived.

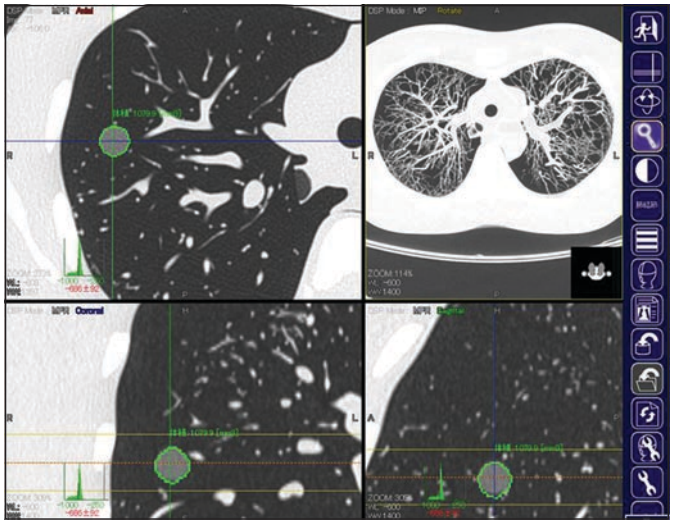

Fig. 3—Chest phantom. Screen display of computer-aided volumetry software used in phantom study shows axial, coronal, and sagittal images and maximum intensity projections. Simulated ground-glass opacity nodule (–630 HU) can be accurately extracted with software.

Nodule selection—One chest radiologist with 21 years of chest CT experience reviewed the records of 211 consecutively registered patients with suspected pulmonary nodules. The patients underwent thin-section helical CT of the chest at our institution during the 36-month period from January 2004 through December 2006. The radiologist, who did not participate in the volume measurement study selected all patients who satisfied the following criteria: GGO nodules that did not exceed 20 mm in the *xy* (transverse) plane, a histologic diagnosis based on findings at thoracic surgery or at CT-guided transcutaneous or bronchoscopic transbronchial biopsy, and absence of consolidation due to the presence of organizing tissues after pneumonia or associated with idiopathic pulmonary fibrosis around the nodules. The last criterion was applied because we found it difficult to define the nodule boundary.

On the basis of the selection criteria, 59 nodules in 59 patients (18 men, 41 women; mean age, 65.4 years; range, 47–79 years) with 40 malignant (BAC, $n = 38$; adenocarcinoma, $n = 2$) and 19 benign nodules (atypical adenomatous hyperplasia, $n = 17$; amyloidosis, $n = 1$; goblet cell metaplasia, $n = 1$) were identified. The mean size in the *xy* (transverse) plane of the 59 nodules was 12.8 ± 4.7 (SD) mm (range, 4.0–20.0 mm). The mean attenuation was –539.6 ± 96.3 HU (range, –744 to –339 HU).

CT—CT scans were obtained with a 4-MDCT scanner (LightSpeed QX/I, GE Healthcare). After routine helical scanning of the whole thorax, thin-slice helical scans with a scan range of approximately 5 cm including the pulmonary nodules were obtained. The scan parameters for routine helical scans were detector collimation, 4 × 2.5 mm; helical pitch (beam pitch), 1.5; slice thickness and interval, 5.0 mm; rotation time, 0.8 second; 120 kVp; 250 mA. The scan parameters for thin-slice helical scans were detector row width, 4 × 1.25 mm; helical pitch, 0.75; slice thickness and interval, 1.25 mm; rotation time, 0.8 seconds; 120 kVp; 160–200 mA. The reconstruction algorithm for thin-slice helical scans was bone plus. Contrast enhancement was not used in any of the 59 nodules. Because the 4-MDCT scanner was replaced with the 64-MDCT scanner in January 2008, we used the 4-MDCT scanner for the clinical and the 64-MDCT scanner for the phantom study.

Volumetry of GGO nodules—Figure 4 shows the screen display of computer-aided volumetry software in the clinical study. Two of the three radiologists (4 and 15 years of experience with chest CT) who participated in the phantom study performed volumetry in the clinical study. Each radiologist performed two volumetry sessions at 1-month or longer intervals. Between the two sessions, the order of case presentation was changed to minimize the learning effect. Before the first session, each radiologist underwent a training session that involved volumetry in three training cases to become familiar with the editing tools of the computer-aided volumetry software because the shape of some of the human nodules was more complex than that of the phantom nodules. The three training cases were not among the 59 cases in the clinical study.

When the GGO nodules were not accurately extracted with the computer-aided volumetry software alone, the two radiologists subjectively edited the

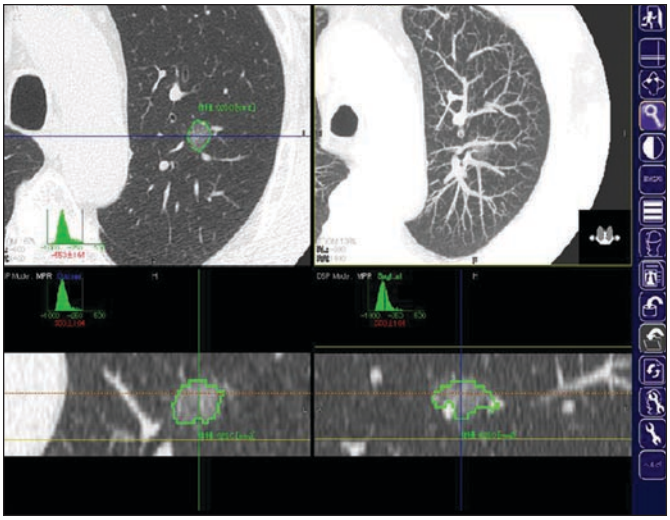

Fig. 4—57-year-old woman with atypical adenomatous hyperplasia. Screen display shows accurate extraction of pure ground-glass opacity nodule (category 1) with computer-aided volumetry software.

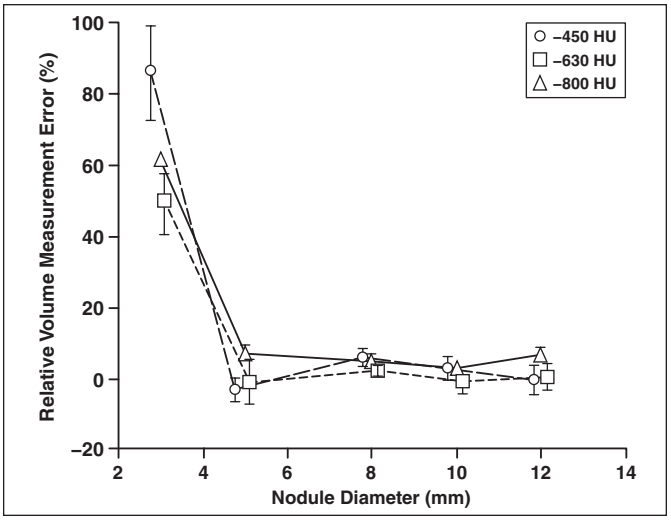

Fig. 5—Graph shows average relative volume measurement error for nodules measuring 3, 5, 8, 10, and 12 mm in diameter with attenuation of –450, –630, and –800 HU. For nodules with attenuation of –450 HU, relative volume measurement error was 85.2% ± 13.5% (SD), –4.1% ± 3.4%, 4.8% ± 2.6%, 1.7% ± 3.4%, and –1.5% ± 4.2%. For nodules with attenuation of –630 HU, relative volume measurement error was 51.1% ± 9.8%, 0.2% ± 6.2%, 3.3% ± 1.4%, 0.2% ± 3.3%, and 1.6% ± 3.7%. For nodules with attenuation of –800 HU, relative volume measurement error was 61.5% ± 4.0%, 7.1% ± 2.1%, 4.8% ± 1.4%, 3.1% ± 1.2%, and 7.0% ± 0.9%.

segmented area using techniques based on mathematic morphology. If an edit was required, we measured the editing time. To investigate whether morphologic nodule characteristics affected the need for editing, the chest radiologist who selected the 59 patients classified the GGO nodules into three categories on the basis of the nature of the nodule margin. Category 1 nodules ($n = 22$) exhibited a well-defined smooth margin; category 2 nodules ($n = 24$) had a well-defined irregular margin; and category 3 nodules ($n = 13$) manifested an ill-defined margin. The radiologist also classified the 59 nodules as partly solid (mixed GGO, $n = 31$) and nonsolid (pure GGO, $n = 28$) according to internal density [1]. The readers recorded whether the GGO nodules were ($n = 12$) or were not ($n = 47$) adjacent to the pleural surface.

Statistical Analysis

All numerical values are reported as mean ± SD. We used Bland-Altman [19] analysis to determine intraobserver and interobserver agreement in the clinical study. We assessed intraobserver and interobserver agreement on nodules < 8 mm and ≥ 8 mm in diameter to evaluate the influence of nodule size. We also assessed agreement on nodules that were or were not subjected to editing to reveal whether and how editing affected the reproducibility of computer-aided volumetry. On the Bland-Altman plots we used the percentage difference of the average of two measured values (relative difference) rather than absolute difference because the variability of the differences increased as the magnitude of the measurements increased.

To determine the frequency of necessary edits (edit rate) required by the morphologic features of the GGO nodules, we performed the chi-square test. To assess the effect of the morphologic features of nodules on edit time, we used Student's *t* test or Tukey multiple comparisons. Variables with a value of $p < 0.05$ were considered to indicate statistically significant differences. Statistical analysis software was used (MedCalc Software, MedCalc; SPSS version 15.0, SPSS).

Results

Phantom Study

The average of the relative volume measurement error values for nodules with a diameter of 3 mm and attenuation of –800, –630, and –450 HU was 61.5%, 51.1%, and 85.2% (Fig. 5). For all nodules 5 mm in diameter or larger, the average ranged from –4.1% to 7.1%. The SD of relative volume measurement error for 3-mm diameter nodules with attenuation values of –800, –630, and –450 HU was 4.0%, 9.8%, and 13.5%. It was 0.9% to 6.2% for all nodules with a diameter of 5 mm or more.

Clinical Study

We were able to perform computer-aided volumetry on all 59 GGO nodules in patients. The mean intraobserver agreement on all GGO nodules was 1.6 ± 11.1% (95% CI, –1.3% to 4.5%) and 1.8 ± 11.5% (95% CI, –1.2% to 4.8%) for observers A and B (Fig. 6, Tables 1 and 2). The mean interobserver agreement for all GGO nodules was 3.2 ± 11.8% (95% CI, 0.1–6.3%) (Fig. 7, Tables 1 and 2). Observer A applied editing to 36 nodules (61.0%) and observer B to 28 nodules (47.5%). Table 3 shows the edit rates for three categories of GGO nodules for the two observers. There was a statistically significant difference in the edit rate of the three categories. There was no statistically significant difference in the edit rates of nonsolid and partly solid GGO nodules. The edit rate for nodules that were adjacent to the pleura was significantly higher than the rate for nodules not adjacent to the pleura.

The mean edit times were 24.1 ± 10.0 seconds and 35.3 ± 12.3 seconds for observers A and B (Table 4). The mean edit time for category 3 nodules was statistically significantly longer than for categories 1 and 2 nodules ($p < 0.01$ and < 0.01 for observer A; $p < 0.01$ and < 0.01 for observer B). The difference in the edit times of the observers was not statistically significant for categories 1 and 2 nodules ($p = 0.92$ and $p = 0.61$). For observer B the time to edit partly solid GGOs was statistically significantly longer than that to edit nonsolid GGOs ($p < 0.01$); for observer A there was no statistically significant difference ($p = 0.36$). The times to edit nodules adjacent to and not adjacent to pleura were not significantly different (observer A, $p = 0.77$; observer B, $p = 0.35$).

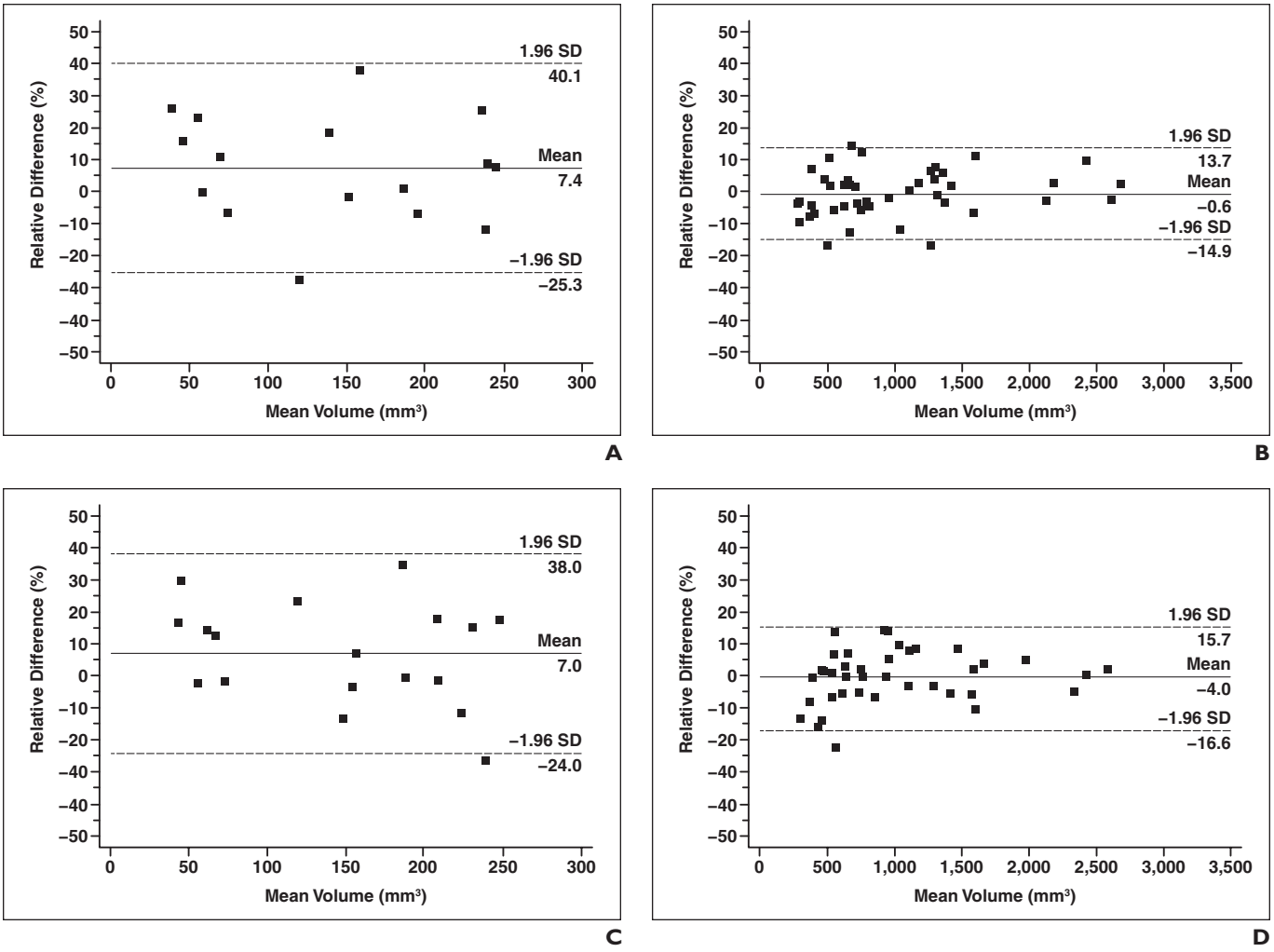

Fig. 6—Intraobserver agreement.
A, Scatterplot shows mean intraobserver agreement on nodules < 8 mm in diameter for observer A was 7.4% ± 16.7% (95% CI, –1.5% to 16.3%); 95% limits of agreement were –25.3% (95% CI, –40.8 to –9.8%) and 40.1% (95% CI, 24.6–55.6%).
B, Scatterplot shows mean intraobserver agreement on nodules ≥ 8 mm in diameter for observer A was –0.6% ± 7.3% (95% CI, –2.8% to 1.7%); 95% limits of agreement were –14.9% (95% CI, –18.7% to –11.0%) and 13.7% (95% CI, 9.8–17.6%).
C, Scatterplot shows mean intraobserver agreement on nodules < 8 mm in diameter for observer B was 7.0% ± 15.8% (95% CI, –0.9% to 14.9%); 95% limits of agreement were –24.0% (95% CI, –37.7% to –10.3%) and 38.0% (95% CI, 24.3–51.7%).
D, Scatterplot shows mean intraobserver agreement on nodules ≥ 8 mm in diameter for observer B was –0.4% ± 8.2% (95% CI, –3.0% to 2.2%); 95% limits of agreement were –16.6% (95% CI, –21.1% and –12.1%) and 15.7% (95% CI, 11.2%–20.2%).

Discussion

Regardless of difficulty in the volumetry of GGO nodules, all GGO nodules in this study were successfully segmented with our computer-aided volumetry software. Our results were better than previously reported volumetry measurements of solid nodules in humans [20, 21]; in those studies, 71–97% of nodules were successfully segmented.

Factors that affect computer-aided volumetry of pulmonary nodules are the algorithm of the volumetry software, the threshold values for nodule extraction, nodule size and attenuation, tube current, and the image reconstruction kernel [15, 16, 22, 23]. The presence of pulmonary vessels, bronchi, or chest wall connecting with the nodule may require manual modification of nodule extraction, and arbitrary manipulation by radiologists may be a factor affecting the accuracy of volumetry. De Hoop et al. [20] assessed the volumetry of solid nodules with six semiautomated software packages. They found manual modification of nodule extraction improved the accuracy of volumetry without significantly affecting reproducibility.

In the evaluation of solid pulmonary nodules, computer-aided volumetry produced only minimal errors and had high measurement reproducibility [12, 13, 23, 24]. Kostis et al. [23], who evaluated computer-aided volumetry of solid nodules in humans, reported that the overall standard measurement error for nodules 2–5 mm, 5–8 mm, and 8–10 mm was 18.5%, 10.6%, and 7.47%. A study conducted by Das et al. [12] revealed that accurate volumetry was possible for simulated solid nodules with a diameter of 5 mm or larger and with a volume greater than 66 mm^3. However, volumetry of GGO nodules is difficult because the attenuation difference between these nodules and normal lung parenchyma is small, and other structures in the lung are visualized in the same attenuation range. An earlier volumetric study

TABLE 1: Comparison of Intraobserver and Interobserver Agreement

Nodules Evaluated	Mean	Upper Limit	Lower Limit
All nodules			
Intraobserver agreement observer A	1.6 (–1.3 to 4.5)	23.3 (18.4 to 28.3)	–20.2 (–25.2 to –15.2)
Intraobserver agreement observer B	1.8 (–1.2 to 4.8)	24.4 (19.2 to 29.5)	–20.7 (–25.8 to –15.5)
Interobserver agreement	3.2 (0.1 to 6.3)	26.4 (21.1 to 31.7)	–20.0 (–25.3 to –14.7)
Nodules < 8 mm in diameter			
Intraobserver agreement observer A	7.4 (–1.5 to 16.3)	40.1 (24.6 to 55.6)	–25.3 (–40.8. to –9.8)
Intraobserver agreement observer B	7.0 (–0.9 to 14.9)	38.0 (24.3 to 51.7)	–24.0 (–37.7 to –10.3)
Interobserver agreement	1.9 (–6.0 to 9.8)	32.2 (18.3 to 46.0)	–28.4 (–42.2 to –14.5)
Nodules ≥ 8 mm in diameter			
Intraobserver agreement observer A	–0.6 (–2.8 to 1.7)	13.7 (9.8 to 17.6)	–14.9 (–18.7 to –11.0)
Intraobserver agreement observer B	–0.4 (–3.0 to 2.2)	15.7 (11.2 to 20.2)	–16.6 (–21.1 to –12.1)
Interobserver agreement	3.7 (0.5 to 6.9)	23.7 (18.3 to 29.2)	–16.3 (–21.8 to –10.8)

Note—Values are percentages. Values in parentheses are 95% CI.

TABLE 2: Influence of Editing on Intraobserver and Interobserver Agreement

Use of Editing	Mean	Upper Limit	Lower Limit
Nodules without editing			
Intraobserver agreement observer A	2.3 (–1.2 to 5.9)	18.3 (12.2 to 24.4)	–13.6 (–19.7 to –7.5)
Intraobserver agreement observer B	0.1 (–3.1 to 3.3)	17.3 (11.7 to 22.8)	–17.1 (–22.6 to –11.5)
Interobserver agreement	3.5 (–0.3 to 7.2)	20.1 (13.6 to 26.6)	–13.1 (–19.6 to –6.6)
Nodules with editing			
Intraobserver agreement observer A	1.1 (–3.2 to 5.4)	26.0 (18.6 to 33.5)	–23.9 (–31.3 to –16.4)
Intraobserver agreement observer B	3.8 (–1.6 to 9.1)	30.8 (21.6 to 40.1)	–23.3 (–32.6 to –14.1)
Interobserver agreement	2.7 (–2.8 to 8.2)	28.2 (18.7 to 37.8)	–22.9 (–32.4 to –13.4)

Note—Values are percentages. Values in parentheses are 95% CI.

[15] on chest phantoms showed significantly higher volume measurement error for GGO than for solid nodules.

In our phantom study, we obtained accurate volumetric measurements for nodules larger than 5 mm in diameter; the mean measurement error for nodules 5 mm or larger was 2.35% (range, –4.14% to 7.13%). Our accuracy rate was equivalent to that in previous studies of solid nodules. In the clinical setting, however, pulmonary nodules are not necessarily round, their margins are not always clear, and they are frequently in contact with adjacent structures, such as the chest wall, pulmonary vessels, and bronchi. In addition, artifacts due to respiratory and cardiac motion are often present on clinical images. The simulated nodules in the chest phantom, however, were round and had clear margins, and there were no motion artifacts. Volumetric measurement therefore may be less accurate in clinical than in phantom studies. We observed measurement variability even in volumetry of simulated GGO nodules in this study. Because the software defines the optimal threshold attenuation within each region of interest specified by the radiologist, the threshold value varies with the size or site of the region of interest. In addition, in some instances editing was needed even for simulated GGO nodules. This factor may account for the measurement variability encountered in our phantom study.

In our clinical investigation, intraobserver and interobserver agreement was relatively high for nodules ≥ 8 mm in diameter. For intraobserver agreement, the 95% limits of agreement were –14.9% and 13.7% for observer A and –16.6% and 15.7% for observer B. For interobserver agreement, the limits of agreement were –16.3% and 23.7% for nodules ≥ 8 mm in diameter. Wormanns et al. [13] obtained excellent results in a study in which intraobserver agreement was –3.9% to 5.7% and interobserver agreement was –5.5% to 6.6% for automated volumetry of clinical solid nodules. Thus volumetric measurements of GGO nodules exhibited larger variability than did solid nodules. Taking into account our intraobserver and interobserver agreement results, the threshold for identifying an increase in the measured volume of a GGO nodule is a 30% increase, equivalent to a 9% increase in nodule diameter. For example, if a 10-mm diameter of a nodule on a baseline scan has increased 1 mm on a follow-up scan, it can be difficult to detect this change with visual assessment. Therefore, we conclude that our results on intraobserver and interobserver agreement are clinically acceptable for early detection of growth of GGO nodules.

We found that intraobserver and interobserver agreement was slightly better for nodules without than for those with editing. We posit, however, that this difference is minimal and acceptable for clinical practice. Although editing based on the subjective judgment of each observer resulted in a few intraobserver and interobserver discrepancies, appropriate editing may be indispensable for accurate volumetry of GGO nodules.

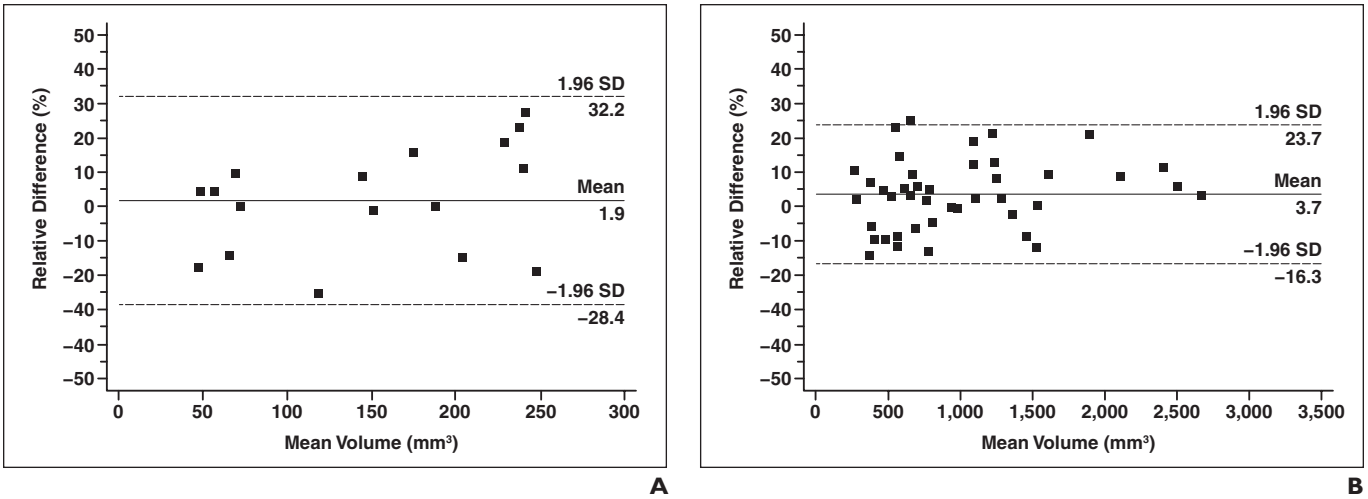

Fig. 7—Interobserver agreement.
A, Scatterplot shows mean interobserver agreement on nodules < 8 mm in diameter was 1.9% ± 15.4% (95% CI, –6.0 to 9.8%); 95% limits of agreement were –28.4% (95% CI, –42.2% to –14.5%) and 32.2% (95% CI, 18.3%–46.0%).
B, Scatterplot shows mean interobserver agreement on nodules ≥ 8 mm in diameter was 3.7% ± 10.2% (95% CI, 0.5%–6.9%); 95% limits of agreement were –16.3% (95% CI, –21.8% to –10.8%) and 23.7% (95% CI, 18.3%–29.2%).

TABLE 3: Edit Rate for Ground-Glass Opacity Nodules According to Morphologic Subtype

	Observer A		Observer B	
Ground-Glass Opacity Subtype	Edit Rate (%)	*p*[a]	Edit Rate (%)	*p*
Margin characteristics		0.03		0.04
Category 1 (22)	54.5 (12)		31.8 (7)	
Category 2 (24)	50.0 (12)		45.8 (11)	
Category 3 (13)	92.3 (12)		76.9 (10)	
Internal density		0.40		0.53
Nonsolid (28)	53.6 (15)		53.6 (15)	
Partly solid (31)	67.7 (21)		41.9 (13)	
Relation to pleura		0.04		0.03
Adjacent to pleura (12)	91.7 (11)		83.3 (9)	
Not adjacent to pleura (47)	53.2 (25)		38.3 (18)	
Total (*n* = 59)	61.0 (36)		47.5 (28)	

Note—Numbers in parentheses are number of patients.
[a]Chi-square test.

In our clinical study, edits were needed for approximately one half of GGO nodules. For category 3 GGO nodules, the edit rate was significantly higher and the edit time significantly longer than for categories 1 and 2 nodules. However, for both observers, the mean edit time for category 3 GGO nodules was shorter than 60 seconds. Furthermore, there was no statistically significant difference in edit time between nodules that were and those that were not adjacent to the pleura. The mean edit time was approximately 30 seconds for both pleura-adjacent and nonadjacent GGO nodules, although the edit rate for nodules adjacent to the pleura was higher. Considering the acceptable length of edit time, we suggest that our computer-aided volumetry software is a practical tool for the measurement of GGO nodules in humans.

One of the most important indicators of malignancy is the growth rate of nodules, commonly expressed as the volume doubling time [13]. Computer-aided volumetric assessment of pulmonary nodules to estimate their growth rate has gained wider acceptance [14, 16]. The reported average BAC doubling time, calculated from the maximal tumor diameter with the Schwartz equation [25] is 457–813 days [8, 11]. In the interpretation of these data, it must be remembered that the reported doubling times for GGO nodules were not based on 3D data. According to Marten et al. [24], the relative mean error of volumetric measurements of pulmonary nodules is significantly higher for manual unidimensional measurements. Intraobserver and interobserver agreement on manual unidimensional measurements was lower than with automated volumetry. Yankelevitz et al. [16] also found that computer-aided 3D volumetry had clear advantages over conventional bilinear 2D measurement for accurate representation of nodular volume. We recommend that the doubling time of pulmonary nodules be reevaluated with highly accurate computer-aided volumetry software that features high reproducibility.

There are inherent problems with volumetry of GGO nodules. First, the size of some BACs with GGO decreased in the course of follow-up owing to the collapse of alveolar spaces, fibrosis, or severe narrowing of the alveolar space [10]. Therefore, even if the size of GGO nodules decreases, malignancy cannot be ruled out. Second, because the cells of BAC with focal GGO manifest replacement growth without marked reduction in the alveolar lumen and without marked thickening of alveolar septa [26], BAC with focal GGO is a relatively soft tumor. Therefore, the volume of BAC with focal GGO may be affected by the lung volume. Furthermore, computer-aided volumetry of GGO nodules seems to be affected by a change in the attenuation of the lung surrounding parenchyma that occurs with inspiratory level. In volume-

TABLE 4: Edit Time for Ground-Glass Opacity Nodules According to Morphologic Subtype

Ground-Glass Opacity Subtype	Observer A		Observer B	
	Edit Time (s)	*p*	Edit Time (s)	*p*
Margin characteristics				
Category 1 (22)	17.5 ± 5.2	Category 1 vs 2, 0.92	29.6 ± 9.9	Category 1 vs 2, 0.61
Category 2 (24)	20.4 ± 9.9	Category 1 vs 3, 0.01	31.4 ± 11.6	Category 1 vs 3, 0.01
Category 3 (13)	33.0 ± 7.4	Category 2 vs 3, 0.01	43.6 ± 10.7	Category 2 vs 3, 0.01
Internal density		0.36		0.01
Nonsolid (28)	22.2 ± 8.8		29.5 ± 8.8	
Partly solid (31)	25.4 ± 10.9		41.9 ± 12.7	
Relation to pleura		0.77		0.35
Adjacent to pleura (12)	24.8 ± 8.0		32.3 ± 9.9	
Not adjacent to pleura (47)	23.7 ± 11.0		36.3 ± 13.4	
Total (*n* = 59)	24.1 ± 10.0		35.3 ± 12.3	

try of focal GGO, the lung volume may have to be taken into consideration.

Debate continues about the treatment of patients with GGO nodules. To our knowledge, no consensus has been reached on whether GGO nodules should be resected or observed. At present there is no definite evidence on the natural history of GGO nodules.

Evaluating the volume-doubling time of GGO nodules with accurate computer-aided volumetry may yield information on tumor activity and lead to better management of GGO nodules. Routine computer-aided volumetry in the follow-up of GGO nodules may also be beneficial. Ikeda et al. [27], who performed 3D analysis of the attenuation within GGO nodules using computer-aided volumetry software for differentiating atypical adenomatous hyperplasia, BAC, and adenocarcinoma, found this method useful. However, even these 3D analyses require high-precision computer-aided volumetry.

During the follow-up of GGO nodules, solid components may appear or grow. According to Henschke et al. [1], the malignancy rate for partly solid GGO nodules was 63%. In adenocarcinoma with partly solid nodules, the ratio of solid to nonsolid parts is related to the prognosis. It is also useful for differentiation of adenocarcinoma subtypes [6, 9]. Therefore, a function for the identification and quantification of solid components within GGO nodules should be added to computer-aided diagnosis at CT follow-up of GGO nodules.

There were several potential limitations to our study. First, because we used a 64-MDCT scanner in the phantom study and a 4-MDCT scanner in the clinical study, the results of the phantom study may not be applicable to the clinical study. Das et al. [12, 28], who compared the accuracy of automated volumetry of solid phantom nodules using CT scanners from different vendors and scanners with different numbers of detectors, concluded that solid nodule volumetry was accurate and that the degree of volume error was acceptable considering that the data were acquired using different scanners. For GGO nodules, however, volumetry with different scanners may lead to a change in the cutoff value and turn out to be a source of variability. A technique that unifies and rectifies the image background between types of scanners is needed. Second, we used a section thickness and interval of 1 mm in the phantom study. In the clinical study, these values were 1.25 mm because the clinical data were collected in a retrospective manner. Goo et al. [29] observed a tendency toward larger volume measurement errors with increasing section thickness. Thus the measured volume in our clinical study may have been overestimated. Third, we did not evaluate interscan variability. Wormanns et al. [13], who used computer-aided volumetry to assess solid pulmonary nodules on two consecutive CT scans on the same day, reported that the 95% limits of agreement were –20.4% and 21.9% (standard error, 1.5%). Gietema et al. [30] also reported similar limits of agreement for interscan variability in volumetry of solid nodules. They suggested that most of the observed measurement variability was attributable to interscan differences. This finding indicates that the effect of interscan variability must be assessed. Last, there may have been selection bias in this study because we selected patients on the basis of the strict criteria described earlier.

We conclude that with our computer-aided volumetry software, volumetry was relatively accurate and that intraobserver and interobserver agreement may be clinically acceptable for the early detection of growth in GGO nodules ≥ 8 mm in diameter. On the basis of our findings we suggest that accurate computer-aided volumetry can play an important role in the follow-up and management of GGO nodules.

References

1. Henschke CI, Yankelevitz DF, Mirtcheva R, McGuinness G, McCauley D, Miettinen OS. CT screening for lung cancer: frequency and significance of part-solid and nonsolid nodules. *AJR* 2002; 178:1053–1057
2. Li F, Sone S, Abe H, MacMahon H, Armato SG 3rd, Doi K. Lung cancers missed at low-dose helical CT screening in a general population: comparison of clinical, histopathologic, and imaging findings. *Radiology* 2002; 225:673–683
3. Park CM, Goo JM, Lee HJ, et al. Focal interstitial fibrosis manifesting as nodular ground-glass opacity: thin-section CT findings. *Eur Radiol* 2007; 17:2325–2331
4. Nakajima R, Yokose T, Kakinuma R, Nagai K, Nishiwaki Y, Ochiai A. Localized pure ground-glass opacity on high-resolution CT: histologic characteristics. *J Comput Assist Tomogr* 2002; 26:323–329
5. Nakata M, Saeki H, Takata I, et al. Focal ground-glass opacity detected by low-dose helical CT. *Chest* 2002; 121:1464–1467
6. Kuriyama K, Seto M, Kasugai T, et al. Ground-glass opacity on thin-section CT: value in differentiating subtypes of adenocarcinoma of the lung. *AJR* 1999; 173:465–469
7. Kim HY, Shim YM, Lee KS, Han J, Yi CA, Kim YK. Persistent pulmonary nodular ground-glass opacity at thin-section CT: histopathologic comparisons. *Radiology* 2007; 245:267–275
8. Aoki T, Nakata H, Watanabe H, et al. Evolution of peripheral lung adenocarcinomas: CT findings correlated with histology and tumor doubling time. *AJR* 2000; 174:763–768
9. Aoki T, Tomoda Y, Watanabe H, et al. Peripheral lung adenocarcinoma: correlation of thin-section CT findings with histologic prognostic factors and survival. *Radiology* 2001; 220:803–809
10. Kakinuma R, Ohmatsu H, Kaneko M, et al. Progression of focal pure ground-glass opacity detected by low-dose helical computed tomography screening for lung cancer. *J Comput Assist Tomogr* 2004; 28:17–23

11. Hasegawa M, Sone S, Takashima S, et al. Growth rate of small lung cancers detected on mass CT screening. *Br J Radiol* 2000; 73:1252–1259
12. Das M, Ley-Zaporozhan J, Gietema HA, et al. Accuracy of automated volumetry of pulmonary nodules across different multislice CT scanners. *Eur Radiol* 2007; 17:1979–1984
13. Wormanns D, Kohl G, Klotz E, et al. Volumetric measurements of pulmonary nodules at multi-row detector CT: in vivo reproducibility. *Eur Radiol* 2004; 14:86–92
14. Kostis WJ, Reeves AP, Yankelevitz DF, Henschke CI. Three-dimensional segmentation and growth-rate estimation of small pulmonary nodules in helical CT images. *IEEE Trans Med Imaging* 2003; 22:1259–1274
15. Ko JP, Rusinek H, Jacobs EL, et al. Small pulmonary nodules: volume measurement at chest CT—phantom study. *Radiology* 2003; 228:864–870
16. Yankelevitz DF, Reeves AP, Kostis WJ, Zhao B, Henschke CI. Small pulmonary nodules: volumetrically determined growth rates based on CT evaluation. *Radiology* 2000; 217:251–256
17. Awai K, Murao K, Ozawa A, et al. Pulmonary nodules: estimation of malignancy at thin-section helical CT—effect of computer-aided diagnosis on performance of radiologists. *Radiology* 2006; 239:276–284
18. Dougherty E. *Digital image processing method.* New York, NY: Dekker, 1994:77–85
19. Bland JM, Altman DG. Statistical methods for assessing agreement between two methods of clinical measurement. *Lancet* 1986; 1:307–310
20. de Hoop B, Gietema H, van Ginneken B, Zanen P, Groenewegen G, Prokop M. A comparison of six software packages for evaluation of solid lung nodules using semi-automated volumetry: what is the minimum increase in size to detect growth in repeated CT examinations. *Eur Radiol* 2009; 19:800–808
21. Goodman LR, Gulsun M, Washington L, Nagy PG, Piacsek KL. Inherent variability of CT lung nodule measurements in vivo using semiautomated volumetric measurements. *AJR* 2006; 186:989–994
22. Winer-Muram HT, Jennings SG, Meyer CA, et al. Effect of varying CT section width on volumetric measurement of lung tumors and application of compensatory equations. *Radiology* 2003; 229: 184–194
23. Kostis WJ, Yankelevitz DF, Reeves AP, Fluture SC, Henschke CI. Small pulmonary nodules: reproducibility of three-dimensional volumetric measurement and estimation of time to follow-up CT. *Radiology* 2004; 231:446–452
24. Marten K, Auer F, Schmidt S, Kohl G, Rummeny EJ, Engelke C. Inadequacy of manual measurements compared to automated CT volumetry in assessment of treatment response of pulmonary metastases using RECIST criteria. *Eur Radiol* 2006; 16:781–790
25. Schwartz M. A biomathematical approach to clinical tumor growth. *Cancer* 1961; 14:1272–1294
26. Noguchi M, Morikawa A, Kawasaki M, et al. Small adenocarcinoma of the lung: histologic characteristics and prognosis. *Cancer* 1995; 75:2844–2852
27. Ikeda K, Awai K, Mori T, Kawanaka K, Yamashita Y, Nomori H. Differential diagnosis of ground-glass opacity nodules: CT number analysis by three-dimensional computerized quantification. *Chest* 2007; 132:984–990
28. Das M, Muhlenbruch G, Katoh M, et al. Automated volumetry of solid pulmonary nodules in a phantom: accuracy across different CT scanner technologies. *Invest Radiol* 2007; 42:297–302
29. Goo JM, Tongdee T, Tongdee R, Yeo K, Hildebolt CF, Bae KT. Volumetric measurement of synthetic lung nodules with multi-detector row CT: effect of various image reconstruction parameters and segmentation thresholds on measurement accuracy. *Radiology* 2005; 235:850–856
30. Gietema HA, Schaefer-Prokop CM, Mali WP, Groenewegen G, Prokop M. Pulmonary nodules: interscan variability of semiautomated volume measurements with multisection CT—influence of inspiration level, nodule size, and segmentation performance. *Radiology* 2007; 245:888–894